# On State Estimation and Fusion with Elliptical Constraints

Qiang Liu and Nageswara S. V. Rao
Computational Sciences and Engineering Division
Oak Ridge National Laboratory
Oak Ridge, TN 37831
Email: {liuq1,raons}@ornl.gov

***Abstract*—We consider tracking of a target with elliptical nonlinear constraints on its motion dynamics. The state estimates are generated by sensors and sent over long-haul links to a remote fusion center for fusion. We show that the constraints can be projected onto the known ellipse and hence incorporated into the estimation and fusion process. In particular, two methods based on (i) direct connection to the center, and (ii) shortest distance to the ellipse are discussed. A tracking example is used to illustrate the tracking performance using projection-based methods with various fusers in the lossy long-haul tracking environment.**

***Index Terms*—Long-haul sensor networks, state estimate fusion, error covariance matrices, nonlinear constraints, elliptical track constraints, root-mean-square-error (RMSE) performance, projection.**

## I. Introduction

Sensor networks have been deployed to support applications in both military and civilian domains [1], [3], in which ground, airborne, or underwater sensors with sensing, data processing, and communication capabilities are tasked for target tracking/monitoring. Typically, target state estimates and error covariances are generated by the sensors and sent to a remote fusion center that fuses the data to obtain global estimates periodically at specified time instants. Long-haul sensor networks usually span a large geographical area and the links between the sensor and the remote fusion center can be fiber-optic, satellite, or underwater acoustic links. The long propagation time and losses over such connections can reduce the amount of useful data available at the fusion center, leading to degraded fusion performance and even failure to meet the system requirements on the overall quality of fused estimates.

In many ground target tracking applications, target dynamics are subject to certain constraints such as those defined by roadways. Constrained estimation and fusion have received increasing attention over the years. In the literature, a unifying modeling framework for equality-constrained dynamic systems is proposed in [15] using a distance-based optimization criterion. Target state-space modeling accounting for constraints has been studied for straight-line and circular tracks respectively in [5] and [6]. In [7], constrained fusion is studied in the context of centralized and distributed incorporation of known linear constraints. [10] and [11] have considered linear constrained fusion in the context of information loss whereas projection-based methods have been studied in [12] for estimation and fusion with circular constraints.

This work continues our investigation of nonlinear constrained fusion with information loss, and as an extension of [12], we focus on elliptical constraints. In particular, we consider two versions of the projection-based solution, using either direct connection to the known ellipse center, or by solving for the shortest-distance point on the ellipse. Overall, we are interested in the effect of various (i) projection methods to incorporate the constraints at the sensors and/or the fusion center; (ii) fusion rules; and (iii) ways the fusion center interpolates missing sensor estimates on fusion performance. Simulation results of a simple tracking example demonstrate the effectiveness of projection-based constrained estimation and fusion under elliptical constraints, and they also show the differences among the solutions with variable losses in the long-haul tracking environment.

The remainder of the paper is organized as follows: Section II reviews constrained system state model. In Section III, we discuss two projection methods to generate constrained state estimates. Several closed-form fusers are briefly discussed in Section IV along with ways to incorporate the elliptical constraints into these fusers. A simulation example is presented in Section V to demonstrate the joint effect of variable information loss, ways to perform projection, and fuser types on tracking performance before the paper concludes in Section VI.

## II. System Model

In this section, after presenting the basic nonlinear state model, namely, the coordinated turn (CT) model, we discuss how to incorporate the known elliptical constraint into the system model to generate the constrained states.

### A. Coordinated Turn (CT) Model

A maneuver (i.e., a turn) usually follows a pattern known as *coordinated turn* (CT) characterized by a near constant turn rate and near constant speeds along both coordinates. Consider a 2D tracking scenario with orthogonal coordinates $\xi$ and $\eta$, and the state estimate $\mathbf{x}$ is composed of position and velocity components along both axes as well as the turn rate component $\Omega$: $\mathbf{x} = \begin{bmatrix} \xi & \dot{\xi} & \eta & \dot{\eta} & \Omega \end{bmatrix}^T$. The evolution of the state vector

Preprint submitted to 2017 IEEE International Conference on Multisensor Fusion and Integration for Intelligent Systems. Received July 20, 2017.

$\mathbf{x}$ is described by the following discretized CT model [2]:

$$\begin{aligned}\mathbf{x}_{k+1} &= \mathbf{F}_k\mathbf{x}_k + \mathbf{u}_k \\ &= \begin{bmatrix} 1 & \frac{\sin\Omega_k T}{\Omega_k} & 0 & -\frac{1-\cos\Omega_k T}{\Omega_k} & 0 \\ 0 & \cos\Omega_k T & 0 & -\sin\Omega_k T & 0 \\ 0 & \frac{1-\cos\Omega_k T}{\Omega_k} & 1 & \frac{\sin\Omega_k T}{\Omega_k} & 0 \\ 0 & \sin\Omega_k T & 0 & \cos\Omega_k T & 0 \\ 0 & 0 & 0 & 0 & 1 \end{bmatrix}\mathbf{x}_k + \mathbf{u}_k, \quad (1)\end{aligned}$$

where $\mathbf{F}$ is the state transition matrix, $T$ is the sampling period[1], the subscript $k$ is the discrete time index, and $\mathbf{u}_k$ is the process noise whose covariance matrix is given by

$$\mathbf{Q}_k = \begin{bmatrix} \tilde{q}_\xi \begin{bmatrix} T^3/3 & T^2/2 \\ T^2/2 & T \end{bmatrix} & \mathbf{0}_{2\times 2} & 0 \\ \mathbf{0}_{2\times 2} & \tilde{q}_\eta \begin{bmatrix} T^3/3 & T^2/2 \\ T^2/2 & T \end{bmatrix} & 0 \\ 0 \quad 0 & 0 \quad 0 & \tilde{q}_\Omega T \end{bmatrix}, \quad (2)$$

in which $\tilde{q}_\xi$ and $\tilde{q}_\eta$ (often assumed to be constant over time) are the power spectral densities (PSDs) of the underlying continuous-time white stochastic process along the axes, and $\tilde{q}_\Omega$ is the noise PSD of the turn rate component.

### B. Elliptical Constraint

Suppose the target trajectory satisfies the following elliptical constraint:

$$\frac{(\xi_k - \xi_c)^2}{a^2} + \frac{(\eta_k - \eta_c)^2}{b^2} = 1, \quad (3)$$

where $(\xi_c, \eta_c)$ is the center of the ellipse, $a$ and $b$ are respectively the radii along the $\xi$ and $\eta$ axes, and for simplicity, the major and minor axes of the ellipsis are parallel to $\xi$ and $\eta$ axes. Taking the derivative of the position constraint, we have the constraint on the velocity as

$$\frac{\xi_k - \xi_c}{a^2}\dot{\xi}_k + \frac{\eta_k - \eta_c}{b^2}\dot{\eta}_k = 0. \quad (4)$$

### C. Generating Constrained States

The constrained target states are generated in two steps: (1) generate states constrained by the unit circle $\xi^2 + \eta^2 = 1$; (2) transform these states to their elliptical constrained counterparts by means of translation and non-uniform scaling.

*1) Constrained States on Unit Circle:* To incorporate the circular constraint into the unconstrained CT model, a method is developed in [6] that utilizes the traveled distance $s_k^c$ along the circular track and its change rate $\dot{s}_k^c$. More specifically, we have the state transition

$$\begin{bmatrix} \xi_{k+1}^c - \xi_c \\ \dot{\xi}_{k+1}^c \\ \eta_{k+1}^c - \eta_c \\ \dot{\eta}_{k+1}^c \end{bmatrix} = \mathbf{F}^c(\Omega_k T + w_k^{s,c}) \begin{bmatrix} \xi_k^c - \xi_c \\ \dot{\xi}_k^c - w_k^{\dot{s},c}(\eta_k^c - \eta_c) \\ \eta_k^c - \eta_c \\ \dot{\eta}_k^c + w_k^{\dot{s},c}(\xi_k^c - \xi_c) \end{bmatrix}, \quad (5)$$

[1]A superscript $T$ always denotes the transpose of a vector or matrix.

where the superscript "c" denotes these variables correspond to the unit circle, $w_k^{s,c}$ and $w_k^{\dot{s},c}$ are the process noise of $s_k^c$ and $\dot{s}_k^c$ respectively, and the matrix

$$\mathbf{F}^c(\Omega_k T + w_k^{s,c}) = \begin{bmatrix} \cos(\Omega_k T + w_k^{s,c})\mathbf{I}_{2\times 2} & -\sin(\Omega_k T + w_k^{s,c})\mathbf{I}_{2\times 2} \\ \sin(\Omega_k T + w_k^{s,c})\mathbf{I}_{2\times 2} & \cos(\Omega_k T + w_k^{s,c})\mathbf{I}_{2\times 2} \end{bmatrix} \quad (6)$$

contains the rotation element using the turning angle $\Omega_k T + w_k^{s,c}$. From Eq. (5), both position and velocity components at time $k+1$ are simply rotations of those at time $k$ that is corrupted by noise. In addition, the updated turn rate component can be updated as

$$\Omega_{k+1} = \frac{\dot{\eta}_{k+1}^c}{\xi_{k+1}^c - \xi_c}, \quad (7)$$

which remains the same for the elliptical track after the transformation to be described below.

It is important to generate these constrained states using an appropriate level of pre-transformation process noise $w_k^s$ so that the overall noise in the elliptical constrained states would reflect the actual process noise level.

*2) Transformation to Elliptical Constrained States:* Now, by simple linear transformations described in the matrix form

$$\begin{bmatrix} \xi_{k+1} \\ \dot{\xi}_{k+1} \\ \eta_{k+1} \\ \dot{\eta}_{k+1} \end{bmatrix} = \begin{bmatrix} a\mathbf{I}_{2\times 2} & \mathbf{0}_{2\times 2} \\ \mathbf{0}_{2\times 2} & b\mathbf{I}_{2\times 2} \end{bmatrix} \begin{bmatrix} \xi_{k+1}^c \\ \dot{\xi}_{k+1}^c \\ \eta_{k+1}^c \\ \dot{\eta}_{k+1}^c \end{bmatrix} + \begin{bmatrix} \xi_c \\ 0 \\ \eta_c \\ 0 \end{bmatrix}, \quad (8)$$

where the first matrix on the right hand side describes the non-uniform scaling along both axes, and the last column vector describes the translation that shifts the center to $(\xi_c, \eta_c)$.

## III. Projection-Based Constrained Estimation

Suppose an unconstrained state estimate has been generated, for instance, by running an extended Kalman Filter (EKF). In this section, we consider two methods to project this estimate onto the ellipse. We have shown in earlier work [12] that both first- and second-order solutions can be used to project an unconstrained estimate onto a circle, with the latter yielding comparable tracking performance while incurring lower computational cost. The second-order projection "normalizes" an unconstrained estimate by finding a point on the circle that has the shortest distance to it, which can be found equivalently by drawing a line connecting the center and the point whose intersection with the circle (near the unconstrained estimate) is the projected position estimate. Due to the eccentricity, however, these two methods are not equivalent for elliptical tracks, and in this section, we discuss both methods separately. Of note is that we can still linearize the elliptical constraints and run piecewise first-order projection, but we focus on the second-order solutions here.


Preprint submitted to 2017 IEEE International Conference on Multisensor Fusion and Integration for Intelligent Systems. Received July 20, 2017.

### A. Direct Connection to Ellipse Center

A line is draw connecting the center and the unconstrained estimate $(\xi_c, \eta_c)$:

$$\eta - \eta_c = \frac{\hat{\eta} - \eta_c}{\hat{\xi} - \xi_c}(\xi - \xi_c) \tag{9}$$

and its intersection with the ellipse Eq. (3) – nearest to the estimate – is the projected position. By solving the system of equations, we have the following projected position estimate:

$$\left(\hat{\xi}^{proj}, \hat{\eta}^{proj}\right) = \begin{cases} \left(\xi_c, \eta_c + b\,\mathrm{sgn}(\hat{\eta} - \eta_c)\right), & \text{if } \hat{\xi} = \xi_c \\ \left(\xi_c + \frac{1}{\sqrt{\frac{1}{a^2} + \frac{1}{b^2}\left(\frac{\hat{\eta}-\eta_c}{\hat{\xi}-\xi_c}\right)^2}} \cdot \mathrm{sgn}(\hat{\xi} - \xi_c), \eta_c + \frac{\hat{\eta}-\eta_c}{\hat{\xi}-\xi_c}(\xi - \xi_c)\right), & \\ \qquad\qquad \text{otherwise} \end{cases} \tag{10}$$

Once this constrained position estimate has been found, we can follow the same method shown in [12], where the projected position components are used to constrain the velocity components. More specifically, the constraint on velocity as in Eq. (4) can be expressed in matrix form as

$$\begin{bmatrix} \frac{\hat{\xi}_k^{proj} - \xi_c}{a^2} & \frac{\hat{\eta}_k^{proj} - \eta_c}{b^2} \end{bmatrix} \begin{bmatrix} \dot{\xi}_k \\ \dot{\eta}_k \end{bmatrix} = 0, \tag{11}$$

which can be seen as a linear constraint and easily incorporated into the unconstrained estimate by the linear projection rule in [12]. For example, if the identity matrix is used as the weighting matrix in the linear projector, then the constrained velocity can be derived as

$$\begin{bmatrix} \hat{\dot{\xi}}_k^{proj} \\ \hat{\dot{\eta}}_k^{proj} \end{bmatrix} = \frac{1}{\left(\frac{\hat{\xi}_k^{proj} - \xi_c}{a^2}\right)^2 + \left(\frac{\hat{\eta}_k^{proj} - \eta_c}{b^2}\right)^2} \times \begin{bmatrix} \left(\frac{\hat{\eta}_k^{proj} - \eta_c}{b^2}\right)^2 & \left(\frac{\hat{\xi}_k^{proj} - \xi_c}{a^2}\right) \cdot \left(\frac{\hat{\eta}_k^{proj} - \eta_c}{b^2}\right) \\ \left(\frac{\hat{\xi}_k^{proj} - \xi_c}{a^2}\right) \cdot \left(\frac{\hat{\eta}_k^{proj} - \eta_c}{b^2}\right) & \left(\frac{\hat{\xi}_k^{proj} - \xi_c}{a^2}\right)^2 \end{bmatrix} \begin{bmatrix} \hat{\dot{\xi}}_k \\ \hat{\dot{\eta}}_k \end{bmatrix}. \tag{12}$$

### B. Shortest Distance to Unconstrained Estimate

The above closed-form solution, albeit simple, is not a true "projection" method per se because we want to invoke certain optimization criteria for projection[2], for example, the minimum Euclidean distance (when the weighting matrix is identity matrix) between the unconstrained estimate and a projected point on the ellipse.

The point on the ellipse Eq. (3) closest to the unconstrained point $(\hat{\xi}_k, \hat{\eta}_k)$ is [4]

$$\left(\hat{\xi}_k^{proj}, \hat{\eta}_k^{proj}\right) = \left(\xi_c + \frac{a^2(\hat{\xi}_k - \xi_c)}{a^2 - t}, \eta_c + \frac{b^2(\hat{\eta}_k - \eta_c)}{b^2 - t}\right), \tag{13}$$

[2]It has been argued in [8] that the projection method itself is somewhat of a greedy approach in that the solution may not always guarantee the true constrained minimum in the original optimization problem formulation

where $t$ is a solution of the equation

$$\frac{a^2(\hat{\xi}_k - \xi_c)^2}{(a^2 - t)^2} + \frac{b^2(\hat{\eta}_k - \eta_c)^2}{(b^2 - t)^2} = 1. \tag{14}$$

In order to solve for $t$, one can multiply both sides of Eq. (14) by $(a^2 - t)^2(b^2 - t)^2$, and then expand and rearrange the equation. Eventually, a quartic equation can be obtained:

$$c_4 t^4 + c_3 t^3 + c_2 t^2 + c_1 t + c_0 = 0, \tag{15}$$

where

$$\begin{aligned} c_4 &= 1, \\ c_3 &= -2(a^2 + b^2), \\ c_2 &= a^4 + 4a^2b^2 + b^4 - a^2(\hat{\xi}_k - \xi_c)^2 - b^2(\hat{\eta}_k - \eta_c)^2, \\ c_1 &= 2a^2b^2\left[(\hat{\xi}_k - \xi_c)^2 + (\hat{\eta}_k - \eta_c)^2 - (a^2 + b^2))\right], \\ c_0 &= a^2b^2\left[a^2b^2 - b^2(\hat{\xi}_k - \xi_c)^2 - a^2(\hat{\eta}_k - \eta_c)^2\right]. \end{aligned} \tag{16}$$

There exist a number of closed-form solutions [13], such as Ferrari's and Descartes' solutions, although one can also use numerical methods find approximate solutions. The process and measurement noises in realistic tracking are small enough when compared to the dimension of the ellipse such that the unconstrained estimate is geographically close enough to the ellipse itself. As such, The 16-term discriminant for the polynomial is empirically negative, meaning the solutions to the above quartic equation consist of two real roots, representing two points on the ellipse that are respectively closest and farthest from the given point, and a pair of complex conjugate roots. One can easily find the projected position estimate by assigning $t$ the real root with the smallest absolute value and plugging it into Eq. (13), and derive the projected velocity components using Eq. (12). As a special case, when the unconstrained position estimate happens to be on the ellipse, one would expect the solution to be $t = 0$ because the projected position is exactly the original unconstrained position estimate.

## IV. Fusion of Constrained Estimates

In this section, we review a few conventional closed-form fusion rules (i.e., for unconstrained estimates), and then discuss how to incorporate the constrained estimates into these rules. Without loss of generality, a two-sensor scenario is considered here since the results can be readily extended to cases involving more sensors.

### A. Fusion Rules

*1) Average Fuser:* The simplest average fuser calculates the arithmetic mean of the sensor estimates as the fuser output:

$$\mathbf{P}_k^G = \frac{1}{2}(\mathbf{P}_k^1 + \mathbf{P}_k^2) \tag{17}$$

$$\hat{\mathbf{x}}_k^G = \frac{1}{2}(\hat{\mathbf{x}}_k^1 + \hat{\mathbf{x}}_k^2), \tag{18}$$

in which the superscript "G" denotes the the global estimate at the fusion center.



Preprint submitted to 2017 IEEE International Conference on Multisensor Fusion and Integration for Intelligent Systems. Received July 20, 2017.

*2) Simple Track-to-Track Fuser:* The simple track-to-track fuser (T2TF) is a convex combination of the sensor estimates as follows [2]:

$$(\mathbf{P}_k^G)^{-1} = (\mathbf{P}_k^1)^{-1} + (\mathbf{P}_k^2)^{-1} \tag{19}$$

$$\hat{\mathbf{x}}_k^G = \mathbf{P}_k^G \left( (\mathbf{P}_k^1)^{-1}\hat{\mathbf{x}}_k^1 + (\mathbf{P}_k^2)^{-1}\hat{\mathbf{x}}_k^2 \right). \tag{20}$$

It is well known that the common process noise results in correlation in the error cross-covariance across sensor estimates. However, it is generally difficult to derive the exact cross-covariances over time; as a result, one may assume that the cross-covariance is negligible in order to apply this simplified fuser, even though the result will be suboptimal.

*3) Fast Covariance Intersection (CI) Algorithm:* Another sensor fusion method without knowledge of the cross-covariance information is the covariance intersection (CI) algorithm. The intuition behind this approach comes from a geometric interpretation of the problem. If one were to plot the covariance ellipses for $\mathbf{P}_F$ (defined as the locus of points $\{\mathbf{y} : \mathbf{y}^T\mathbf{P}_F^{-1}\mathbf{y} = c\}$ where $c$ is some constant), the ellipses of $\mathbf{P}_F$ are found to always contain the intersection of the ellipses for $\mathbf{P}_1$ and $\mathbf{P}_2$ for all possible choices of $\mathbf{P}_{12}$ [9]. The method is characterized by the weighted convex combination of sensor covariances:

$$(\mathbf{P}_k^G)^{-1} = \omega_1(\mathbf{P}_k^1)^{-1} + \omega_2(\mathbf{P}_k^2)^{-1} \tag{21}$$

$$\hat{\mathbf{x}}_k^G = \mathbf{P}_k^G \left( \omega_1(\mathbf{P}_k^1)^{-1}\hat{\mathbf{x}}_k^1 + \omega_2(\mathbf{P}_k^2)^{-1}\hat{\mathbf{x}}_k^2 \right), \tag{22}$$

where $\omega_1, \omega_2 > 0$ ($\omega_1 + \omega_2 = 1$) are weights to be determined (e.g., by minimizing the determinant of $\mathbf{P}_k^G$). A fast CI algorithm has been proposed in [14] where the weights are found based on an information-theoretic criterion so that $\omega_1$ and $\omega_2$ can be solved for analytically as follows:

$$\omega_1 = \frac{D(p_1, p_2)}{D(p_1, p_2) + D(p_2, p_1)}, \tag{23}$$

where $D(p_A, p_B)$ is the Kullback-Leibler (KL) divergence from $p_A(\cdot)$ to $p_B(\cdot)$, and $\omega_2 = 1 - \omega_1$. When the underlying estimates are Gaussian, the KL divergence at time $k$ can be computed as

$$D_k(p_i, p_j) = \frac{1}{2}\left[ \ln \frac{|\mathbf{P}_k^j|}{|\mathbf{P}_k^i|} + \mathbf{d}_{k,i\to j}^T (\mathbf{P}_k^j)^{-1}\mathbf{d}_{k,i\to j} + Tr(\mathbf{P}_k^i(\mathbf{P}_k^j)^{-1}) - n \right], \tag{24}$$

where $\mathbf{d}_{k,i\to j} = \hat{\mathbf{x}}_k^i - \hat{\mathbf{x}}_k^j$, $n$ is the dimensionality of the state, and $|\cdot|$ denotes the determinant.

### B. Fusion Rules with Constrained Estimates

When the sensors do not perform projection themselves, i.e., the fuser inputs are all unconstrained estimates, the fuser can simply perform conventional fusion, followed by one-step correction using either of the projection methods described above, which can be considered "centralized" projection. If one or more sensors send their self-projected estimates to the fusion center, as in "distributed" projection, since only nonsingular covariance matrices can be used as inputs to the T2TF, fast-CI, or any fuser that requires the inverse of the error covariances, then the sensors can still send their unconstrained covariances along with constrained estimates to the fusion center. The implementation of these schemes will be discussed in more detail in the tracking example presented below.

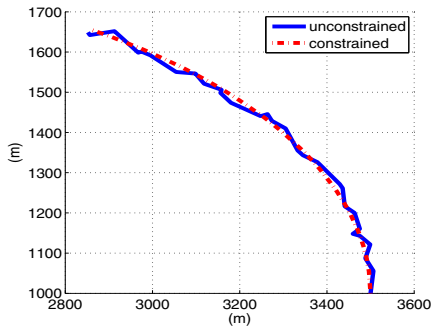


**Fig. 1:** Unconstrained and constrained position estimates

## V. Constrained Fusion with Information Loss

We study the position estimate root-mean-squared error (RMSE) performances of the constrained estimation and fusion methods described in the previous section using a simple tracking example with elliptical constraints. The effect of (i) projection method, (ii) projection-fusion implementation, (iii) fuser type, and (iv) information loss on constrained fusion performance are considered.

### A. Simulation Setup

The center of the elliptical track is $(\xi_c, \eta_c) = (2000, 1000)$ m with radii along the axes $a = 1500$ m and $b = 800$ m. A total of 5000 simulations are run for each test scenario. The initial state of the target is generated around $\mathbf{x}_0 = (\xi_c + a, \eta_c, 0, v_0, v_0/a)$ where $v_0 = 25$ m/s; that is, the initial position is centered around $(\xi_c + a, \eta_c)$ and the mean magnitude of the initial velocity is $v_0$. The target state is generated for a total of 60 seconds using the constrained target model presented in Section II.

Two sensors are used to observe the constrained motion where the (position) measurements are generated as

$$\mathbf{H}^{(1)} = \mathbf{H}^{(2)} = \begin{bmatrix} 1 & 0 & 0 & 0 & 0 \\ 0 & 0 & 1 & 0 & 0 \end{bmatrix}$$

$$\mathbf{V}^{(1)} = \text{diag}\{20^2, 20^2\} \quad \mathbf{V}^{(2)} = \text{diag}\{15^2, 15^2\},$$

where $\mathbf{H}$ and $\mathbf{V}$ are the measurement matrix and noise covariance respectively. Each sensor is initialized with a sufficiently large error covariance and runs EKF on top of the CT model with appropriate parameters, i.e., the process noise PSDs $\tilde{q}_\xi$, $\tilde{q}_\eta$, and $\tilde{q}_\Omega$ that reflect the level of (scaled) process noise $w_k^s$ in Eq. (6), the latter of which is generated here as a zero-mean normal random variable with a standard deviation of 2 mm. The estimation interval is set to be $T = 2$ s.


Preprint submitted to 2017 IEEE International Conference on Multisensor Fusion and Integration for Intelligent Systems. Received July 20, 2017.

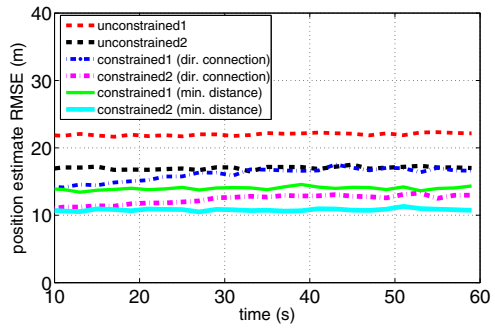


**Fig. 2:** Position RMSE of unconstrained and constrained estimates at each sensor

### B. Performance

*1) Sensor Performance:* First we want to look at the state estimation performance of both sensors. Depending on whether a sensor incorporates the elliptical constraint Eq. (3) into its estimation process, we have the position RMSEs of both unconstrained and constrained estimates plotted in Fig. 2; and for the latter, we have the "dir. connection" option representing the method where the constrained position estimate is the intersection of a center-to-point ray and the ellipse, and the "min. distance" option representing the method in which the projected estimate is the solution of a quartic function and has the minimum distance to the given point. Fig. 1 shows sample trajectories of both the original/unconstrained and constrained position estimates (with minimum-distance projection) generated by Sensor 1 during one run of the simulation. From the plots in Fig. 2, we can see that by incorporating the constraints, the estimation accuracy performance can be significantly improved at both sensors, where the position RMSEs can be reduced by approximately 30% with the direct connection method and 40% with the minimum distance method when compared against their unconstrained counterparts. We will focus on the performance of the second method in the remainder of paper since it in general provides further improvement in reducing tracking errors.

In what follows, we consider fusion performance with either centralized or distributed projection in the context of long-haul communication loss. Loss can effectively reduce the number of successfully delivered estimates to the fusion center, which in turn would need to apply prediction (using the same CT model) based on previously available sensor estimates and such predicted values would then be used as input for subsequent fusion. In general, more prediction steps are needed with increasing link loss rates to interpolate the missing estimates, thereby increasing the overall estimation and fusion errors, as will be shown below.

*2) Fuser Performance with Centralized Projection:* In Fig. 3, fusion performances under 0%, 25%, and 50% losses using unconstrained are plotted. The notation "-proj" indicates the projection step carried out by the fusion center after fusing unconstrained estimates. From the plots, the errors of these constrained fused estimates are lower than their unconstrained counterparts; for example, for the simple track-to-track fuser (T2TF), consistently yielding the best performance followed by CI and average fusers, the reduction in position RMSEs is generally around 40%. Interestingly, the performance gaps among the fusers also increase significantly with higher link loss rates, demonstrating the advantage of the T2TF in its lowest tracking errors and less sensitivity with respect to increased loss.

*3) Fuser Performance with Distributed Projection:* Finally, we repeat the above simulations, but now with projected sensor estimates and nonsingular unconstrained sensor error covariances as the fuser input. For cases with nonzero loss, the fusion center can either use its predicted estimates directly (based on previous sensor estimates) to interpolate the missing estimates, or it can perform an extra projection step in between prediction and fusion steps (as shown in "-proj" in the plots) to guarantee the position estimate input to the fuser is indeed on the ellipse. From Fig. 4, we observe that without the intermediate fuser projection step, while the position RMSEs of the fused estimates are, not surprisingly, smaller than those of the unconstrained fused estimates, the former errors can be higher than their counterparts with centralized projection in Fig. 3; the extra step to force the predicted estimates onto the constraint can indeed guarantee largely comparable performance between the centralized and distribution projection methods even with increasing link loss.

*4) Discussions:* Information loss results in increased tracking error across the board as expected. It also appears necessary for the fusion center to perform the projection step either before or after the final fusion step with increasing loss, regardless of constrained/unconstrained nature of the individual sensor estimates. For example, for T2TF and CI fusers, even with 50% loss, the fusion center, after performing its own projection, can still yield more accurate position estimates compared to the original unconstrained sensor estimates in Fig. 2.

In addition, the exact distance from the unconstrained estimate to the projected point on ellipse may also be taken into account by the fusion center. With increasing sensor measurement noise and/or possible non-zero bias, the closer an unconstrained estimate is to the center (equivalently, farther away from the ellipse), the higher the probability that it is projected to a point on the ellipse farther away from the ground truth, and the effect can be more pronounced near the minor axis of the ellipse especially when the eccentricity becomes larger. It would seem preferable to have the fusion center carry out the final projection step, i.e., centralized projection, to reduce the overall uncertainty in sensor measurement quality and also reduce the additional computational requirement on the part of the sensors, e.g., to solve the quartic equations.

## VI. Conclusions

We explored constrained estimation and fusion in tracking a target whose motion is constrained by elliptical tracks. The effect of long-haul link loss and various ways to implement projection-based estimation and fusion were also investigated for different fuser types. Future directions may include fusion


Preprint submitted to 2017 IEEE International Conference on Multisensor Fusion and Integration for Intelligent Systems. Received July 20, 2017.

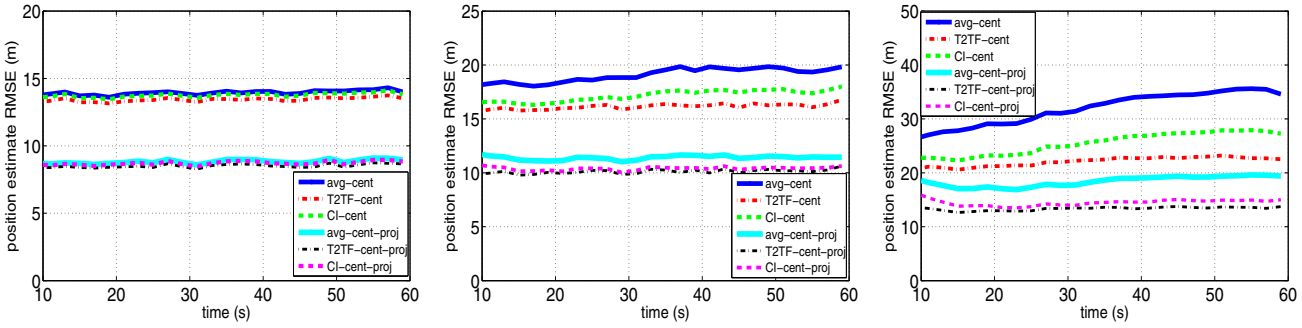


(a) 0% loss (b) 25% loss (c) 50% loss

**Fig. 3:** Position RMSE of fused estimates with centralized projection

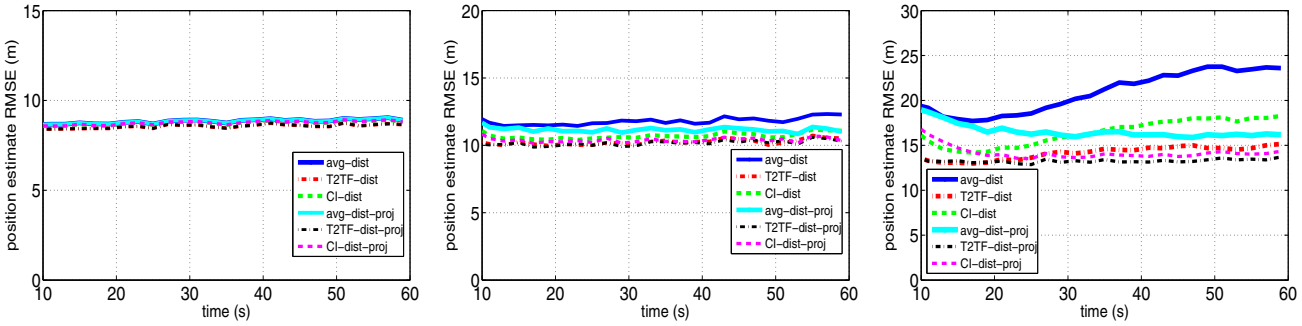


(a) 0% loss (b) 25% loss (c) 50% loss

**Fig. 4:** Position RMSE of fused estimates with distributed projection

of state estimates under more complex motion constraints and/or sensor measurement models with varying levels of bias. Also of interest are constrained estimation and fusion with partially known and/or time-varying constraint parameters, for which a more adaptive multiple-model approach can be pursued to account for increased system uncertainty.

## ACKNOWLEDGMENT

This work is funded by the Mathematics of Complex, Distributed, Interconnected Systems Program, Office of Advanced Computing Research, U.S. Department of Energy, and SensorNet Project of Office of Naval Research, and is performed at Oak Ridge National Laboratory managed by UT-Battelle, LLC for U.S. Department of Energy under Contract No. DE-AC05-00OR22725.

## REFERENCES

[1] I. F. Akyildiz, W. Su, Y. Sankarasubramaniam, and E. Cayirci. A survey on sensor networks. *Communications Magazine, IEEE*, 40(8):102–114, Aug. 2002.

[2] Y. Bar-Shalom, P. K. Willett, and X. Tian. *Tracking and Data Fusion: A Handbook of Algorithms*. YBS Publishing, 2011.

[3] W. Boord and J. B. Hoffman. *Air and Missile Defense Systems Engineering*. CRC Press, Boca Raton, FL, 2016.

[4] J. M. Borwein and J. D. Vanderwerff. *Convex Functions: Constructions, Characterizations and Counterexamples*. Encyclopedia of Mathematics and its Applications. Cambridge University Press, 2010.

[5] Z. Duan and X. R. Li. Constrained target motion modeling – part i: straight line track. In *Proc. 16th International Conference on Information Fusion (FUSION)*, pages 2161–2167, Istanbul, Turkey, Jul. 2013.

[6] Z. Duan and X. R. Li. Constrained target motion modeling – part ii: circular track. In *Proc. 16th International Conference on Information Fusion (FUSION)*, pages 2153–2160, Istanbul, Turkey, Jul. 2013.

[7] Z. Duan and X. R. Li. Multi-sensor estimation fusion for linear equality constrained dynamic systems. In *Proc. 16th International Conference on Information Fusion (FUSION)*, pages 93–100, Istanbul, Turkey, Jul. 2013.

[8] R. J. Hewett, M. T. Heath, M. D. Butala, and F. Kamalabadi. A robust null space method for linear equality constrained state estimation. *Signal Processing, IEEE Transactions on*, 58(8):3961–3971, Aug. 2010.

[9] S. J. Julier and J. K. Uhlmann. A non-divergent estimation algorithm in the presence of unknown correlations. In *Proceedings of the American Control Conference*, volume 4, pages 2369–2373, Albuquerque, NM, Jun. 1997.

[10] Q. Liu and N. S. V. Rao. Projection-based linear constrained estimation and fusion over long-haul links. In *Proc. 12th International Conference on Multisensor Fusion and Integration for Intelligent Systems (MFI)*, pages 365–370, Baden-Baden, Germany, Sep. 2016.

[11] Q. Liu and N. S. V. Rao. State estimation and fusion over long-haul links under linear constraints. In *Proc. 19th International Conference on Information Fusion (FUSION)*, pages 1937–1944, Heidelberg, Germany, Jul. 2016.

[12] Q. Liu and N. S. V. Rao. Projection-based circular constrained state estimation and fusion over long-haul linkss. In *Proc. 20th International Conference on Information Fusion (FUSION)*, Xi'an, China, Jul. 2017.

[13] S. L. Shmakov. A universal method of solving quartic equations. *International Journal of Pure and Applied Mathematics*, 71(2):251–259, 2011.

[14] Y. Wang and X. R. Li. Distributed estimation fusion with unavailable cross-correlation. *Aerospace and Electronic Systems, IEEE Transactions on*, 48(1):259–278, Jan. 2012.

[15] L. Xu, X. R. Li, Z. Duan, and J. Lan. Modeling and state estimation for dynamic systems with linear equality constraints. *Signal Processing, IEEE Transactions on*, 61(11):2927–2939, Jun. 2013.



Preprint submitted to 2017 IEEE International Conference on Multisensor Fusion and Integration for Intelligent Systems. Received July 20, 2017.